AD-A159 737 ELECTRON IRRADIATION OF P-TYPE MERCURY CADMIUM TELLURIDE(U) NAVAL POSTGRADUATE SCHOOL MONTEREY CA D G MORRAL JUN 85 1/1

UNCLASSIFIED F/G 20/12 NL

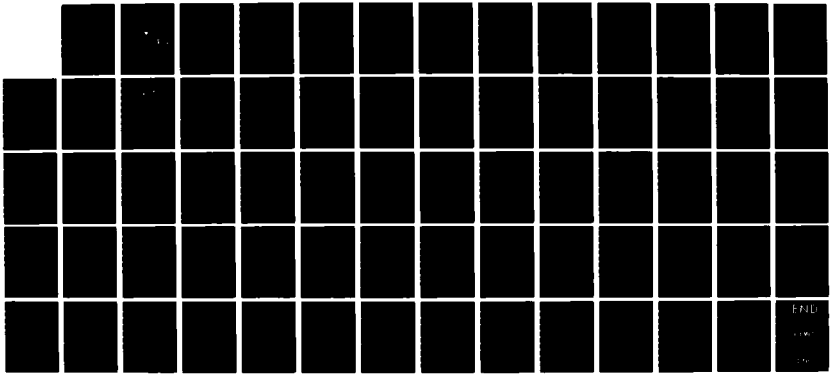

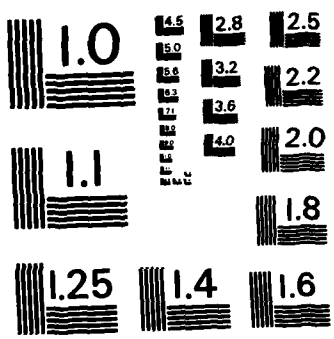

NAVAL POSTGRADUATE SCHOOL
Monterey, California

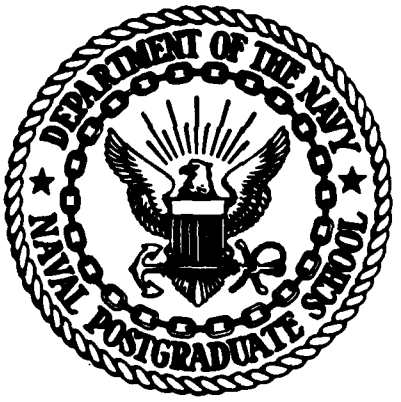

THESIS

ELECTRON IRRADIATION OF p-TYPE
MERCURY CADMIUM TELLURIDE

by

Dennis Gilbert Morral

June 1985

Thesis Advisor: K. C. Dimiduk

Approved for public release; distribution is unlimited

SECURITY CLASSIFICATION OF THIS PAGE (When Data Entered)

REPORT DOCUMENTATION PAGE		READ INSTRUCTIONS BEFORE COMPLETING FORM
1. REPORT NUMBER	2. GOVT ACCESSION NO. AD-A159 237	3. RECIPIENT'S CATALOG NUMBER
4. TITLE (and Subtitle) Electron Irradiation of p-Type Mercury Cadmium Telluride		5. TYPE OF REPORT & PERIOD COVERED Master's Thesis; June 1985
		6. PERFORMING ORG. REPORT NUMBER
7. AUTHOR(s) Dennis G. Morral		8. CONTRACT OR GRANT NUMBER(s)
9. PERFORMING ORGANIZATION NAME AND ADDRESS Naval Postgraduate School Monterey, California 93943-5100		10. PROGRAM ELEMENT, PROJECT, TASK AREA & WORK UNIT NUMBERS
11. CONTROLLING OFFICE NAME AND ADDRESS Naval Postgraduate School Monterey, California 93943-5100		12. REPORT DATE June 1985
		13. NUMBER OF PAGES 66
14. MONITORING AGENCY NAME & ADDRESS(if different from Controlling Office)		15. SECURITY CLASS. (of this report) Unclassified
		15a. DECLASSIFICATION/DOWNGRADING SCHEDULE

16. DISTRIBUTION STATEMENT (of this Report)

Approved for public release; distribution is unlimited.

17. DISTRIBUTION STATEMENT (of the abstract entered in Block 20, if different from Report)

18. SUPPLEMENTARY NOTES

19. KEY WORDS (Continue on reverse side if necessary and identify by block number)

electron irradiation, radiation effects, mercury cadmium telluride, HgCdTe

20. ABSTRACT (Continue on reverse side if necessary and identify by block number)

30 Mev electrons were used to irradiate samples of p-type $Hg_{1-x}Cd_x$ Te to study radiation induced changes in conductivity versus temperature. Samples were held below 95°K while irradiated with doses between 4×10^{13} electrons/cm^2 and 6×10^{15} electrons/cm^2. Little or no change in conductivity was detected for the lower dose levels. Conductivity steadily decreased with increasing dose level, showing a 50% decline at

DD FORM 1 JAN 73 1473 EDITION OF 1 NOV 65 IS OBSOLETE

S N 0102-LF-014-6601

SECURITY CLASSIFICATION OF THIS PAGE (When Data Entered)

20. (continued)

100°K for the maximum dose. The decrease in conductivity was smaller at higher temperatures. Approximately two hour post-irradiation temperature excursions up to 300°K, resulted in a 25% restoration of the conductivity at 100°K. The mobility of the samples, irradiated at the maximum dose level showed a 3 to 6 fold increase, while the majority carrier concentration decreased by a factor of 7 to 10 times the pre-irradiation values. All samples irradiated with dose levels above 1 x 10^{15} electrons/cm^2, converted from p to n-type at 295°K, but remained p-type at 77°K. It was hypothesized that radiation induced donor defect levels in the conduction band were responsible for the reported changes.

Approved for public release; distribution is unlimited

Electron Irradiation of p-Type Mercury Cadmium Telluride

by

Dennis Gilbert Morral
Lieutenant Commander, United States Navy
B.S., United States Naval Academy, 1972

Submitted in partial fulfillment of the
requirements for the degree of

MASTER OF SCIENCE IN PHYSICS

from the

NAVAL POSTGRADUATE SCHOOL
June 1985

Author: Dennis G. Morral
Dennis Gilbert Morral

Approved by: Kenneth C. Dimiduk
K. C. Dimiduk, Thesis Advisor

Harold Walters
D. L. Walters, Second Reader

G. E. Schacher
G. E. Schacher, Chairman, Department of Physics

J. N. Dyer
J. N. Dyer, Dean of Science and Engineering

ABSTRACT

30 Mev electrons were used to irradiate samples of p-type $Hg_{1-x}Cd_xTe$ to study radiation induced changes in conductivity versus temperature. Samples were held below 95°K while irradiated with doses between 4×10^{13} electrons/cm^2 and 6×10^{15} electrons/cm^2. Little or no change in conductivity was detected for the lower dose levels. Conductivity steadily decreased with increasing dose level, showing a 50% decline at 100°K for the maximum dose. The decrease in conductivity was smaller at higher temperatures. Approximately two hour post-irradiation temperature excursions up to 300°K, resulted in a 25% restoration of the conductivity at 100°K. The mobility of the samples, irradiated at the maximum dose level showed a 3 to 6 fold increase, while the majority carrier concentration decreased by a factor of 7 to 10 times the pre-irradiation values. All samples irradiated with dose levels above 1×10^{15} electrons/cm^2, converted from p to n-type at 295°K, but remained p-type at 77°K. It was hypothesized that radiation induced donor defect levels in the conduction band were responsible for the reported changes.

TABLE OF CONTENTS

ACKNOWLEDGEMENT

I would like to thank my Thesis Advisor, Dr. Kathryn C. Dimiduk, for her assistance on all phases of this project, over the past year.

Dr. Paul Newman, Dr. J. Bajaj, and Dr. Dennis Edwall, at Rockwell International Science Center, provided advice and direction which improved the quality of the experimental work.

I would like to express a special thanks to my friend, Dr. Shigeo Okubo who provided assistance in the writing of this report, and to his lovely wife, Kai, who proofed the report, and more importantly kept me well fed throughout the entire project.

I. INTRODUCTION

A. OVERVIEW

Mercury Cadmium Telluride alloys are widely used as infrared detectors in a variety of space, military, and industrial systems. In many of the environments in which they are deployed, they could conceivably be subject to high levels of radiation from nuclear weapons or the Van Allen radiation belts. This research project was undertaken to study the irradiation effects of high energy electrons on several of the important structural, electrical, and optical properties of p-type Mercury Cadmium Telluride (HgCdTe). The experiments conducted for this research were capable of measuring changes in electrical properties only. Optical and structural properties were studied in order to enhance the understanding of this alloy. The HgCdTe samples were Liquid Phase Epitaxially (LPE) grown p-type $Hg_{.68}Cd_{.32}Te$. They were provided by the Rockwell International Science Center, Thousand Oaks, California and irradiated at the Naval Postgraduate School (NPS) Linear Accelerator Laboratory, Monterey, California.

Chapter I of this report provides a brief summary of earlier irradiation studies at NPS and three previous studies on p-type HgCdTe. Chapter II deals with the theoretical aspects of several topics which are considered pertinent to

this research. The theoretical aspects are separated into three categories: structural, electrical, and optical. Chapter III describes experimental procedures including equipment design and sample preparation. Chapter IV discusses the data collected and how it was analyzed. Lastly, Chapter V provides conclusions drawn from both the theoretical investigations and data analysis, followed by recommendations for future work at NPS.

B. IRRADIATION STUDIES AT THE NPS

Two electron irradiation studies on semiconductors have been conducted at NPS. Ness (1984) [Ref. 1] studied the electron irradiation effects on several types of light-emitting diodes (LEDs). Bauer (1985) [Ref. 2] studied the effects of high energy electron irradiation on the electrical properties of Cadmium Telluride (CdTe). CdTe is the substrate on which HgCdTe is grown and therefore HgCdTe irradiation research was considered a logical follow-on to Bauer's work. The HgCdTe work also tested the capabilities of the irradiation equipment designed by Bauer with an eye towards improvements for future irradiation studies.

C. EARLIER INVESTIGATIONS OF P-TYPE HgCdTe

Since the 1960's, research has been conducted on the effects of irradiation on the structural, electrical, and optical properties of HgCdTe alloys. Most of the research has concentrated on n-type material. However, several

studies on irradiation effects on p-type material have been conducted.

Melngailis et al. (1972) [Ref. 3] studied the effects of electron irradiation on the electrical and optical properties of samples kept below 25°K during irradiation. This study reported an increase of 4 orders of magnitude in conductivity when irradiated with 2.5 Mev electrons to doses of 4.7×10^{15} electrons/cm^2. Post-irradiation annealing resulted in almost complete restoration of the electrical transport properties with the major portion of this annealing taking place at temperatures from 50° to 75°K. The samples used for this experiment had x values of 0.22 and 0.31. After irradiation all samples were found to have been converted from p to n-type.

Malon et al. (1975) [Ref. 4] conducted experiments on p-type material with the samples maintained at 80°K during 5 Mev electron irradiation. The conductivity decreased with increasing dose levels and p to n-type conversion took place when dose levels were above 7.5×10^{15} electrons/cm^2. Annealing resulted in a significant degree of restoration centered around 250°K with almost all electrical properties restored for anneal temperatures of 340°K.

Voitsekhovskii et al. (1981) [Ref. 5] examined the changes in carrier lifetime brought about by 2.3 Mev electron irradiation of p-type material held at 300°K. The x value of these samples was 0.195 and 0.205 and p to n-type conversion

was reported for dose levels above 5 x 10^{17} electrons/cm^2. Post-irradiation annealing resulted in significant restoration of the electrical properties. The most prominent annealing for these samples took place between 360° to 430°K.

The experiments conducted at the NPS on p-type HgCdTe differed from previous electron irradiation research in that samples had an x value of 0.32 and dose levels were achieved with 30 Mev electrons. How the findings of previous studies compare with and pertain to the NPS results will be dealt with in Chapter IV.

II. THEORETICAL ASPECTS OF MERCURY CADMIUM TELLURIDE

A. IMPORTANCE OF HgCdTe

The research and development of the HgCdTe alloy has resulted from the need for a material capable of thermal imaging in the 8-12 micrometer response range at 77°K operation. Mercury Cadmium Telluride alloys represented by the formula Hg_{1-x} Cd_x Te exhibit semiconducting properties over much of their composition range. The variable x in the formula is known as the composition variable or mole fraction and defines the relative amounts of mercury and cadmium in the alloy. These alloys act as semimetals at a composition variable of x=0 and semiconductors when x=1.0. Their forbidden bandgaps vary between 0.0 to 1.605 electron volts as x increases from 0.17 to 1.0. HgCdTe's long wavelength photoconductive capability has resulted in its widespread use as a infrared photodetector in numerous applications.

More recently HgCdTe's use as photovoltaic detectors has been developed. In this capacity n-type material is created on p-type material creating a p-n junction. High energy electron irradiation is not useful in fabricating p-n junctions because the range of high energy electrons is large compared to the thickness of the semiconductor material. The importance of high energy irradiation research is in the area of radiation hardening of devices which use p-type HgCdTe and

due to their application could be subject to high energy radiation.

B. STRUCTURAL PROPERTIES AND RADIATION EFFECTS

HgCdTe alloys are II-VI compounds which are isomorphous with the zincblende structure. The zincblende structure is Face Centered Cubic (FCC) with four anion interstitial sites within the unit cell and four cation sites representing the normal FCC lattice positions. In HgCdTe compounds each Te ion has four nearest neighbors which may be either Cd or Hg as shown in Fig. 1(a).

Quantum mechanical calculations indicate that a perfectly periodic lattice would not interact with an electromagnetic field. However due to lattice vibrations, impurities, and defects which cause stresses in the lattice structure the electric field is not in resonance with the crystal. Collisions can then occur between the electrons and the lattice structure, causing an energy transfer between the electrons and the atomic cores which form the lattice.

Imperfections in the crystal control important physical properties such as mobility, carrier concentration and type. Annealing the structure in a Te-rich solution depletes the lattice metal resulting in a p-type material. Annealing in a Hg-rich solution results in a n-type material. It is believed that three types of defects are responsible for type determination; Hg and Te vacancies and Hg interstitials.

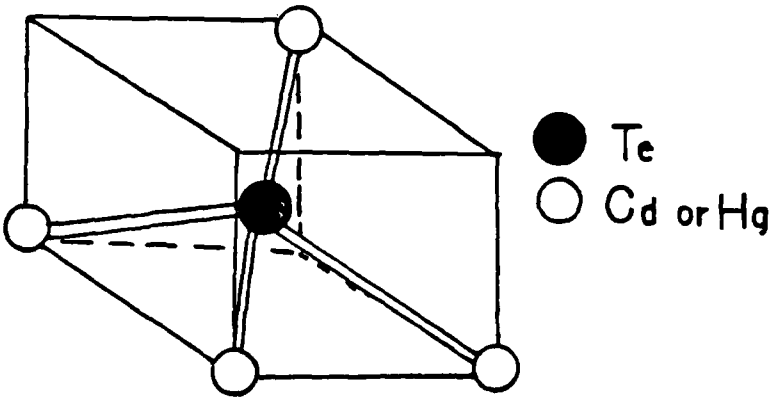

(a) FCC Crystal Structure

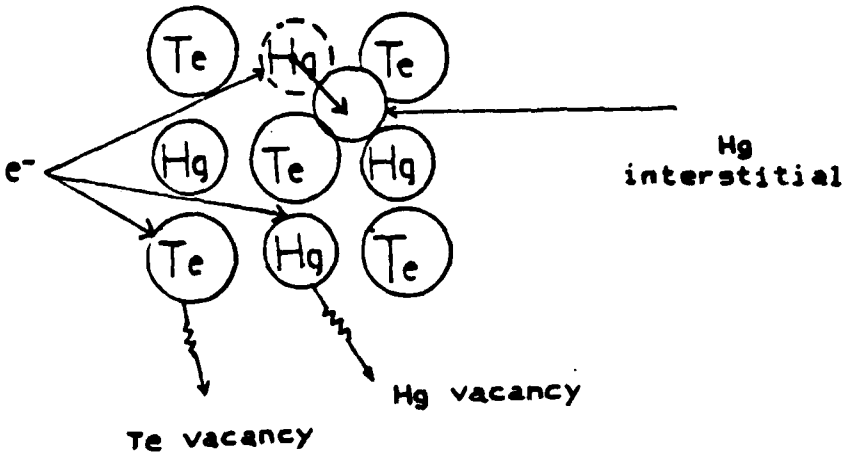

(b) Types of Displacement Damage due to Electron Irradiation

Fig. 1 Crystal Lattice Structure of HgCdTe and Displacement Damage Mechanisms

[Ref. 6] Experimental evidence points toward Hg vacancies as being the cause for the formation of p-type material. [Ref. 6] The Hg vacancies act as acceptor states whose energy depends on the composition variable x.

Electron irradiation can also cause defects in the crystal structure. Two fundamental effects of high energy electron irradiation on the lattice are ionization and displacement damage. Ionization damage results from knocking orbital electrons from an atom to form ionized atoms and free electrons. This type of damage is temporary since normally the electrical design of the device can quickly sweep these away, unless they occur in a surface insulator. Displacement damage refers to the physical damage to a crystal lattice produced by knocking an atom from its normal lattice position to another position. In the process of displacement damage, electrons collide with the lattice atom, transferring their energy to the atom causing it to move either entirely out of the crystal or into interstitial sites. In both cases a vacancy is created. Displacement damage is illustrated in Fig. 1(b). The observed type conversion of p to n-type caused by electron irradiation is believed to be the result of either Te vacancy or Hg interstitial defects. [Ref. 6]

Annealing or thermal defect modification is a process which can change the crystal defects over a period of time. This is usually accomplished by raising the semiconductor's temperature and holding it there for a set period of time.

Annealing results in a reduction of damage due to the recombination of crystal vacancies and interstitials allowing the crystal to return to its original condition. It is difficult in a particular situation to determine if the observed reduction in damage is due to a vacancy-interstitial annihilation or the formation of a different defect complex. If the new defect complex is ineffective in changing the properties that are usually a sign of damage such as carrier concentration, mobility, and lifetime then it may be undistinguishable from a vacancy-interstitial annihilation. [Ref. 7] If a defect is near the conduction or valence band, then it may be ineffective in causing radiation damage due to its allowable energy states. Evidence for this theory comes from observations that for some experiments, increases in temperature have actually caused an increase in damage effects. [Ref. 7] Therefore it appears that annealing is a reordering of defect mechanisms that include vacancy-interstitial annihilation. [Ref. 7]

C. ELECTRICAL PROPERTIES

1. Extrinsic p-Type Semiconductor

The samples of HgCdTe used for this research were p-type extrinsic semiconductor material. A brief review of the band theory of solids will help explain the transport properties of this material.

In the band theory of solids the highest energy band that is completely filled is the valence band. The next higher band whether occupied or not is referred to as the conduction band. In order for an electron to contribute to the electrical conductivity of the material, it must be in the conduction band. As shown in Fig. 2(a) an electrical conductor has a partially filled conduction band. When a potential difference is applied, these electrons can move and a current can be measured. An insulator, as shown in Fig. 2(b), has an empty conduction band. Due to the large forbidden energy gap the probability that an electron can gain enough energy to move up into the conduction band is small, and the material exhibits low conductivity. A semiconductor is a material which has a conductivity somewhere between a conductor and an insulator. In a pure intrinsic semiconductor, Fig. 2(c), the forbidden energy gap is relatively small, and, therefore, even at room temperatures some of the valence electrons can acquire sufficient thermal energy to jump across the forbidden gap to the conduction band. The sites that the electrons leave behind are positively charged and referred to as holes. When an electric or magnetic field is applied, nearby electrons can move into these empty states, creating a current. Therefore, these holes will move in an opposite direction to the electrons. Since the energy band diagrams are drawn so that the energy

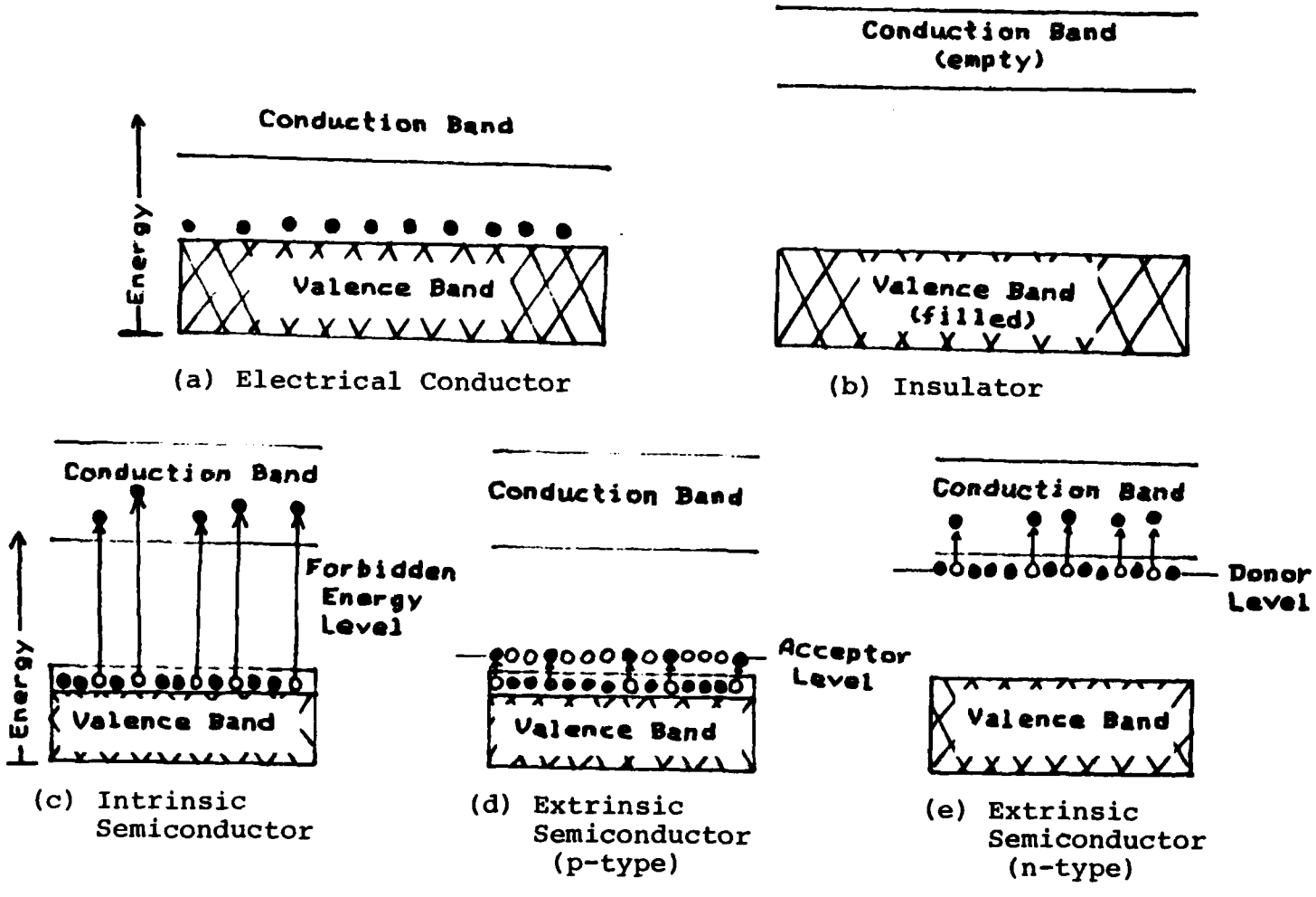

Fig. 2 Energy Band Diagram for Describing Electrical Conduction in Solids
(• electrons, o holes, ▨ filled band)

of an electron moving upwards is increasing, the energy of a hole increases as we move downward on the same diagram. Another point to keep in mind when dealing with holes is that they cannot exist in free space and can only be discussed in conjunction with the energy bands of a solid. In an intrinsic semiconductor, Fig. 2(c), the excitation of an electron into the conduction band always creates an electron hole pair, and, therefore, the number of electrons in the conduction band always equals the number of holes in the valence band.

When two semiconductor materials of differing carrier densities are brought together, alteration of the conduction band properties occurs. In order to produce the different types of semiconductors, small amounts of impurity are added to the pure semiconductor. These impurities are usually substitutional impurities in that they occupy the lattice sites in place of the atoms of the pure semiconductor. This process is referred to as doping, and these semiconductors are known as extrinsic or impurity-activated semiconductors. An impurity atom which contributes a hole to the semiconductor is known as an acceptor. If most impurities are of the acceptor type, the number of holes in the valence band is much greater than the number of electrons in the conduction band, and essentially only one type of charge carriers, in this case holes, contributes to the conductivity as shown in Fig. 2(d). Holes are referred to as the majority

carriers, electrons as the minority carriers, and the material is said to be p-type since most of the current is carried by the positively charged holes.

If most of the impurities are of the donor type, then electrons are the majority carriers, and the material is called n-type as shown in Fig. 2(e). Since the samples for this project were all p-type, Fig. 2(d) best illustrates the pre-irradiation situation, although after type conversion Fig. 2(e) would apply.

2. Bandgap and Photoconductivity

The importance of the bandgap to an infrared detector can be illustrated by a simple review of the photoeffect. The energy of a photon can be expressed as

$$E = h\nu = \frac{hc}{\lambda} \qquad (1)$$

where h is Planck's constant, ν is the frequency, c is the velocity of light, and λ is the wavelength. If an incident photon collides with an electron it can transfer its energy to the electron and the photon ceases to exist. As can be seen from equation (1) the energy of the photon is directly proportional to the frequency and inversely proportional to the wavelength. If the incident photons impart sufficient energy to valence electrons they can move to the conduction band, creating electron-hole pairs, resulting in a photon induced change in conductivity. Obviously, there will exist

a minimum photon energy which will allow the valence electrons to move up into the conduction band. Since low photon energy is the same as low frequency which equates to long wavelength, there exists a long wavelength cutoff which can be expressed as

$$\lambda_c = \frac{1.24}{E_g} \tag{2}$$

where E_g is the forbidden energy gap in electron volts and λ_c is the wavelength cutoff in micrometers (μm).

The forbidden energy gap of $Hg_{1-x}\ Cd_x\ Te$ alloys has been experimentally determined for a large number of x values. An analytic expression for the energy bandgap derived from this data is

$$E_g = 1.59\ x - 0.25 + 5.233\ (10^{-4})\ T\ (1 - 2.08\ x) + 0.327\ x^3 \tag{3}$$

where E_g is the energy bandgap in electron volts (eV), x is the composition variable and T is the absolute temperature. [Ref. 8] For a composition variable of x = 0.32 which was used in this thesis, equation (3) yields a bandgap energy of 0.282 eV at 77°K. Evaluation of the bandgap over a large temperature range indicates a nearly linear dependence.

Evaluating equation (1) with a E_g of 0.282 results in a long wavelength cutoff of about 4.4 μm. If a longer

wavelength detector is desired, a material with a narrower bandgap must be chosen.

3. Hall Measurements

Hall measurements provide a technique for determining resistivity, mobility, and majority carrier concentration. This section provides a discussion of Hall effect measurements, including a description of how this information can be used to detect p to n-type conversion, followed by a brief summary of the Van de Pauw technique. The Van de Pauw technique is a method for making Hall measurements on material of arbitrary shape.

A circuit setup for measuring Hall effects is shown in Fig. 3(a). Fig. 3(b) applies if the majority carriers are holes. Fig. 3(c) applies if the majority carriers are electrons. The following development will be for positive carriers since this research dealt mostly with p-type material.

If we set up an electric field as shown in Fig. 3(b), then a voltage difference will exist between points b and d and a current will flow as shown. The current density J and electric field can then be related by

$$J = \sigma E \qquad (4)$$

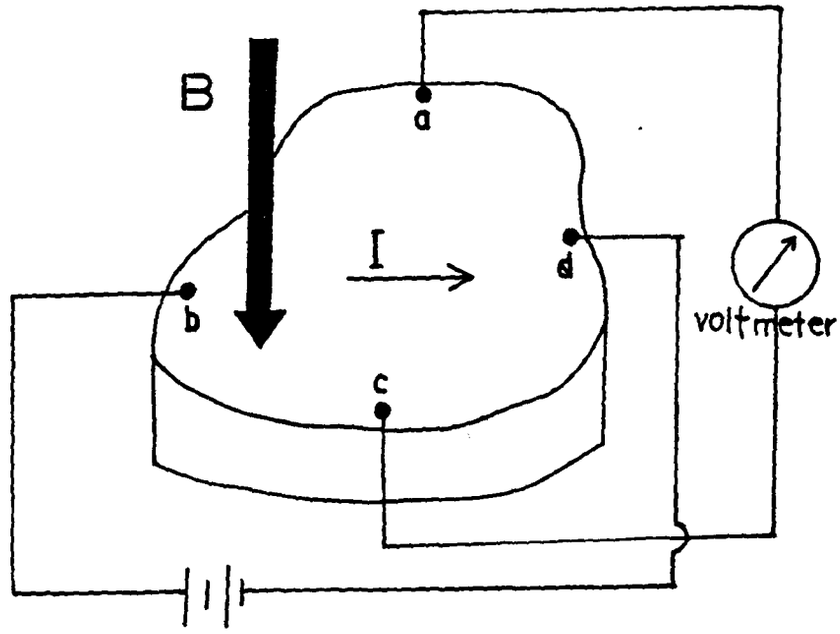

(a) Apparatus for Observing Hall Effects

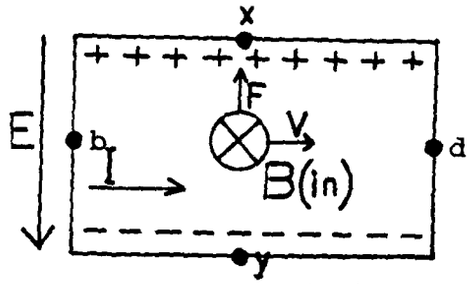

(b) Current Carried by Positive Charges (holes)

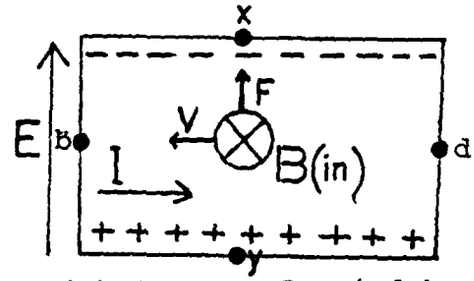

(c) Current Carried by Negative Charges (electrons)

Fig. 3 Hall Measurements

where σ is the conductivity. The next step is to find the drift velocity, v_d, which is the net carrier velocity when a field is applied. This is accomplished by equating the impulse (Force x Time) applied to an electron during its free flight between collisions with the momentum gained by the electron in the same amount of time. This can be expressed as

$$qE\tau = M_p^* v_d \tag{5}$$

where q is the electronic charge which is positive for this case, τ is the mean time between collisions for the holes, and M_p^* is the effective mass. Solving equation (5) for the drift velocity yields

$$v_d = \frac{q\tau E}{M_p^*} \tag{6}$$

Equation (6) provides a relationship between the drift velocity V_d and the electric field E. The proportionality factor $Q\tau/M_p^*$ is known as the hole mobility and represented by

$$\mu_p = \frac{q\tau}{M_p^*} \tag{7}$$

From equations (6) and (7) it can be seen that

$$V_d = \mu_p E \tag{8}$$

This indicates that mobility describes how strongly the motion of a hole is influenced by an electric field. The current density in the direction of the applied electric field is equal to the product of the charge on each hole times the velocity over all the holes which can be expressed as

$$J = q p V_d = (q p \mu_p) E \tag{9}$$

The term in the parenthesis is called the conductivity of the holes and can be expressed as

$$\sigma = q \mu_p p \tag{10}$$

where p is the concentration of holes.

If the magentic field is created at right angles to the sample it will exert a deflecting force F which points upward in Fig. 3(b), as can be seen from

$$\vec{F}_b = q\vec{V} \times \vec{B} \tag{11}$$

This force applies to each moving charge. The upward movement can be clearly seen from equation (11). In Fig. 3(b) the product of the positive charge q and $\vec{v} \times \vec{B}$ results in a $\vec{F}_B$ vector in the upward direction. In Fig. 3(c) the $\vec{v} \times \vec{B}$ vector points in the downward direction but the negative sign of the electron reverses the direction of the $\vec{F}_B$ vector. This movement of charge carriers creates a transverse Hall potential difference which can be represented by V_{xy}. The sign of the charge carriers can be determined by the sign of the Hall potential difference. If the carriers are positive, the potential will be higher at point x than at y and if the carriers are negative, the potential will be lower at point x than at y.

In order to apply the above theory to material of arbitrary shape, a technique developed by Van der Pauw is required. [Ref. 9] For the Van der Pauw technique four small contacts are made along the circumference of the sample as shown in Fig. 4. The resistance $R_{ab,\,cd}$ and $R_{bc,\,da}$ can then be measured as well as t, the thickness of the sample. This information is used to find the resistivity ρ of the material which is expressed by

$$\rho = \frac{\pi t}{\ln 2} \frac{(R_{ab,cd} + R_{bc,da})}{2} f\left(\frac{R_{ab,cd}}{R_{bc,da}}\right) \qquad (12)$$

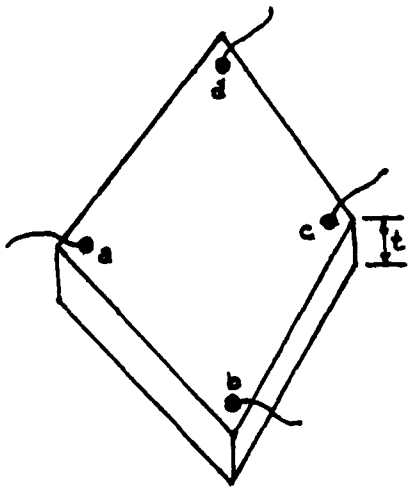

Figure 4. Diagram of Sample for Explaining Van der Pauw Technique

where f(R) is a special function which essentially takes into the account the unsymmetrical factors related to the shape of the sample. [Ref. 9] The Hall mobility can then be determined by measuring the change of the resistance $\Delta R_{bd,\ ac}$ when a magnetic field $\vec{B}$ is applied perpendicular to the sample. The Hall mobility is given by

$$\mu_H = \frac{t}{D} \frac{\Delta R_{bd,ac}}{\rho} \tag{13}$$

The hole concentration in cm^{-3} can be determined by

$$p = \frac{6.28 \times 10^{8}}{\rho \mu_H} \tag{14}$$

4. Mobility, Scattering, and Lifetime

The free carriers in a semiconductor would not interact and exchange energy with a stationary, perfect crystal lattice. However, at any temperature above absolute zero, the atoms of the lattice vibrate, interrupting the periodicity of the lattice, allowing the carriers to interact. If this was the only mechanism operating, then as the temperature increased, causing more lattice vibrations, one would expect more interactions between the carriers and the crystal, slowing the carriers down, and thus decreasing mobility.

When dopants are added to the intrinsic material, they cause lattice distortions. Unlike lattice vibrations, this effect will decrease as temperature increases. The reason for this is that as temperature increases, the carriers are moving faster and spend less time near the impurities, causing them to be less effectively scattered. [Ref. 10] Therefore, if impurity scattering is the dominant mechanism, mobility will increase with increasing temperature.

Scattering can also occur due to crystal defects which develop during manufacture or as a result of irradiation. Irradiation was used in this research to produce defects. Defect levels can act as either hole or electron traps. While a carrier is in a trap, it is not available for conduction, and, therefore, it is normally expected that traps will reduce mobility. Another point

is that carrier concentration depends on the difference between the concentrations of the two types of dopant impurities, usually represented by $N_d - N_a$. Scattering which controls mobility on the other hand, depends on the sum of the ionized impurities, $N_d + N_a$. This implies that the mobility can decrease significantly, although the dopant concentration of the majority carrier remains constant.

Obviously, predictions of the expected mobility can be difficult since all or any combination of the above defect mechanisms can be present simultaneously. If the mobility of each of these mechanisms can be determined independently, the overall mobility can be predicted by adding the inverse values of each. Since mobility is inversely proportional to carrier lifetime, the process which causes the smallest lifetime will dominate the mobility. Lifetime is defined as the length of time a carrier exists from the time it is generated until it recombines. This process is known as recombination.

5. Recombination

Three recombination mechanisms are generally used to describe how thermodynamic equilibrium is achieved in a semiconductor. The recombination mechanisms are called Shockley-Read, Auger, and radiative recombination. These mechanisms are illustrated in Fig. 5. The Shockley-Read mechanism usually occurs as a result of impurities and

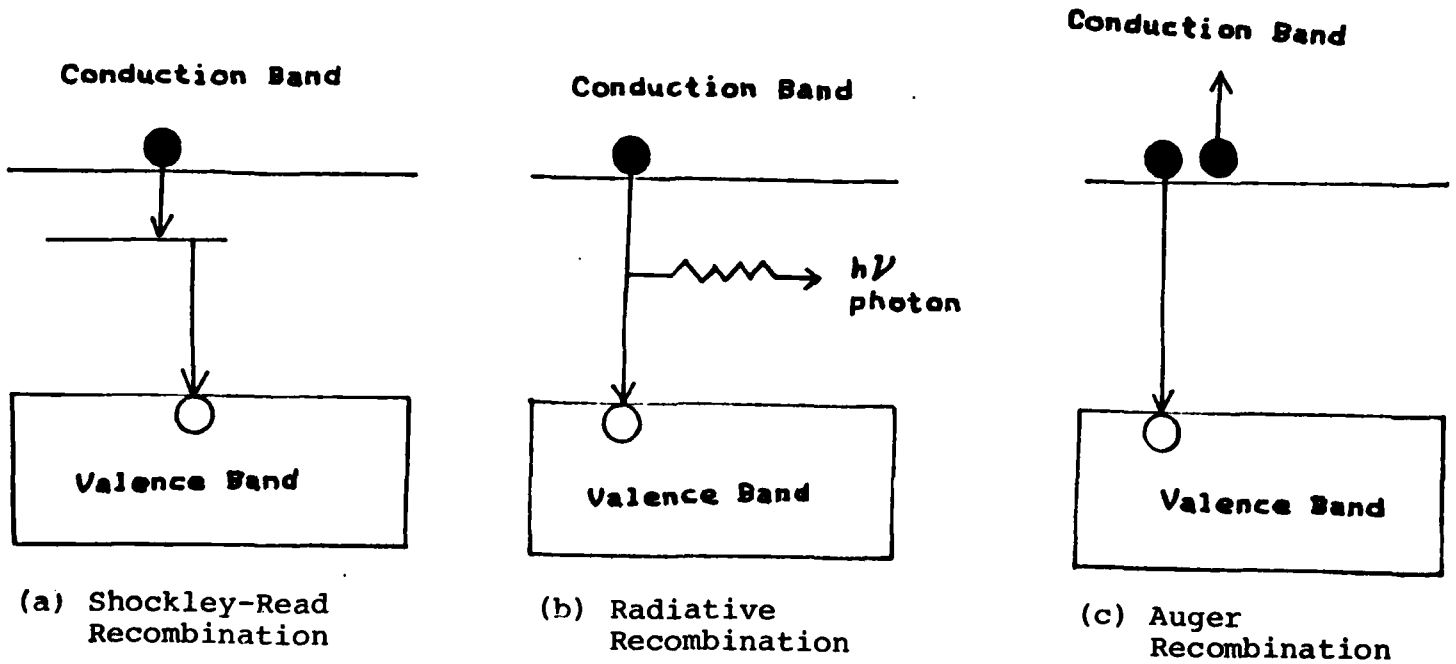

Fig. 5 Mechanisms Controlling Electron-hole Recombination in HgCdTe

lattice defects, which produce energy levels within the bandgap. These levels can behave as recombination centers which provide locations in the bandgap where holes and electrons can recombine which is referred to as electron-hole annihilation. If the Shockley-Read mechanism is dominant then the carrier lifetime will be proportional to the number of recombination centers, which is proportional to the number of defects or impurities. As previously discussed, defects and impurities can be altered by doping or irradiation. The other two mechanisms, radiative and Auger, are not a function of the crystal defects and are referred to as intrinsic mechanisms, since they are determined by the electronic band structure of the semiconductor. As illustrated in Fig. 5(b) the radiative recombination involves a photon which is emitted when the recombination takes place, and is inversely proportional to the total concentration of free electrons and holes. The other type of intrinsic mechanism, Auger, involves an electron to electron interaction in which an electron combines with a hole, and a third electron absorbs the recombination energy and moves up in the energy band. Since this involves three particles interacting, Auger recombination is highly dependent on carrier density. The probability that three particles will be at the same place simultaneously is much less than for just two, and, therefore, radiative and Shockley-Read mechanisms normally dominate the recombination process.

The effect of defect traps can also be examined with a probabilistic approach. There is a certain probability that an electron will exist at a certain energy level or recombination center. There is also a certain probability that a hole will exist at the recombination center. If a trap is created in the structure which captures holes then the probability that a hole will be at the recombination center and recombine with an electron is decreased, causing the lifetime of the carrier to increase. As a result of this alone one would expect mobility to increase. However, while the carrier is in the trap, it is not available for conduction, which has a decreasing effect on the mobility. Since increasing the lifetime but decreasing the availability of the carriers counteracts each other, what the overall effect on mobility will be is not readily apparent.

D. OPTICAL PROPERTIES

Photon detectors may be made for operation either in the photoconductive (PC) or photovoltaic (PV) mode. The semiconductor properties of HgCdTe make it suitable for use in both modes. If a valence electron acquires enough energy from an incident photon to create an electron-hole pair, photon induced variation in conductivity can result. An external potential difference must be supplied in order to measure this change. A device which works on this principle is referred to as a photoconductive detector.

The other type of photon detector utilizes a p-n junction and is known as a photovoltaic detector. Photovoltaic detectors are produced by bringing p and n-type materials together. The large difference in electron concentrations causes electrons to flow from the n-type to the p-type material and the holes from the p-type to the n-type material. As the carriers move they leave behind uncompensated dopant atoms near the junction, which results in the buildup of an electric field in this junction. In this arrangement, when electron-hole pairs are produced by a photon, they are acted upon by the electric field at the junction, causing them to flow. The flow of carriers creates a photovoltage which can be measured. One advantage of photovoltaic detectors is that they do not need an external power supply to create voltage. This simplifies the design of optical systems using photovoltaic elements.

One measure of how various parameters influence the optical effectiveness of a photoconductive detector is responsivity. Responsivity is a measure of the detector output per unit input. With an extrinsic material with only one type of charge carrier, for instance p-type where holes dominate, the conductivity is given by the equation which was developed earlier.

$$\sigma = q \mu_p p \qquad (15)$$

where q is the positive charge of the carrier, μ_p is the hole mobility and p is the number of free carriers per unit volume generated by thermal excitation. This equation holds in the absence of any photon excitation. If the photons are at the correct frequency, then upon striking the detector, they will increase the number of free carriers. At steady state this increase of free carriers represented by Δp can be written as

$$\Delta p = n\tau \tag{16}$$

where n is the number of excitations per second per unit volume and τ is the lifetime of these carriers. If the detector has an area of 1 cm^2 and thickness x in cm, then

$$n = \frac{\eta Q}{x} \tag{17}$$

where η is the quantum efficiency (number of charge carriers produced per photon) and Q is the incident photon flux. The responsivity is proportional to the fractional change in conductivity per incident photon. [Ref. 7] By combining equations 15, 16, and 17, and letting Q = 1 for one incident photon, responsivity can be expressed as

$$R = \frac{\Delta\sigma}{\sigma} = \frac{\eta\tau q \mu_p}{x\sigma} \tag{18}$$

As can be seen from this equation, in order to obtain a high responsivity we need to maximize quantum efficiency, carrier lifetime, and mobility while minimizing thickness of the sample and the conductivity.

III. EXPERIMENTAL PROCEDURES

This chapter describes the experimental procedures used to conduct the electron irradiation studies of HgCdTe. The procedures will be divided into four sections: pre-irradiation, irradiation, post-irradiation, and dose level calculations. The switching boxes used to control the voltage and current levels to the sample, the integration of the equipment, and the computer program used to conduct the experiments were designed as a thesis project by Paul Bauer at the Naval Postgraduate School. [Ref. 2] Equipment design in this report will be dealt with only as necessary to clarify experimental procedures. Reference 2 can be referred to if a detailed description of this equipment is desired.

A. PRE-IRRADIATION MEASUREMENTS

Samples of p-type Hg_{1-x} Cd_x Te were obtained from Rockwell International Science Center. The Liquid Phase Epitaxial technique in a horizontal boat was used by Rockwell to manufacture these samples. [Ref. 11] The samples ranged in size from an area of about 0.15 to 0.25 cm^2 and in thickness from .0014 to .0018 centimeter. Immediately prior to attaching contacts, the samples of substrate were etched in a bromine-methanol solution for about ten seconds to remove oxides. Four contacts were made to the samples by

placing one small drop of gold chloride solution along each side, followed by indium which was melted, using a fine point soldering iron at low heat. Fine silver wires were then attached to the indium contacts and the sample was mounted on a thin piece of sapphire using a drop of General Electric 7031 varnish. The function of the sapphire was to provide electrical insulation between the sample and the aluminum mounting block. A solution of phosphorous powder and clear lacquer was painted around the edge of the sapphire, being careful not to touch the sample. This phosphorous solution glowed when irradiated by the electron beam and provided some insurance that the sample was centered in the beam.

Next, the sample was attached to a 4 point probe via 4 fine silver wires. The probe was placed in a small dewar which was mounted between the poles of an electromagnet. The probe leads were connected to two multimeters, a current source, and a switching box, which allowed voltage and current readings to be taken on the sample. A programmable HP-85 computer was used to calculate the resistivity of the sample from the voltage and current readings, which were automatically read from the meters. The program was based on the Van der Pauw technique and was written by Bauer. Ref. 2. contains a copy of this program.

In preparation for determining the Hall potential difference, the electromagnet was activated and set at

4 KGauss. The probe was placed between the poles of the electromagnet and data was collected to determine the Hall mobility, Hall resistivity and carrier concentration, which were calculated and printed out by the computer. These Hall measurements were taken with the sample immersed in liquid nitrogen (77°K) and at room temperature (295°K).

In order to set up for irradiation measurements of conductivity versus temperature, the sample was removed from the probe. The above equipment, with the exception of the electromagnet, was transported to the NPS Linear Accelerator Lab. The arrangement of the apparatus used to mount the sample inside the Linac vacuum chamber is illustrated in Fig. 6. The sample which was still mounted on the sapphire backing was attached directly to the Al block using thermally conductive paste. The four silver wires were soldered to contacts which were attached to a plastic grid to provide insulation between the contacts and the Al block. A Chromel-Alumel thermocouple was attached to the block directly below the sample and secured, using thermal paste. A small copper core resistive wire heater was coated at the surface with thermal paste and bolted to the bottom of the Al block. A target screen was mounted on one side of the Al block, perpendicular to the sample. The top of the block was coated with a thermal paste and attached to the bottom of the nitrogen dewar. The dewar

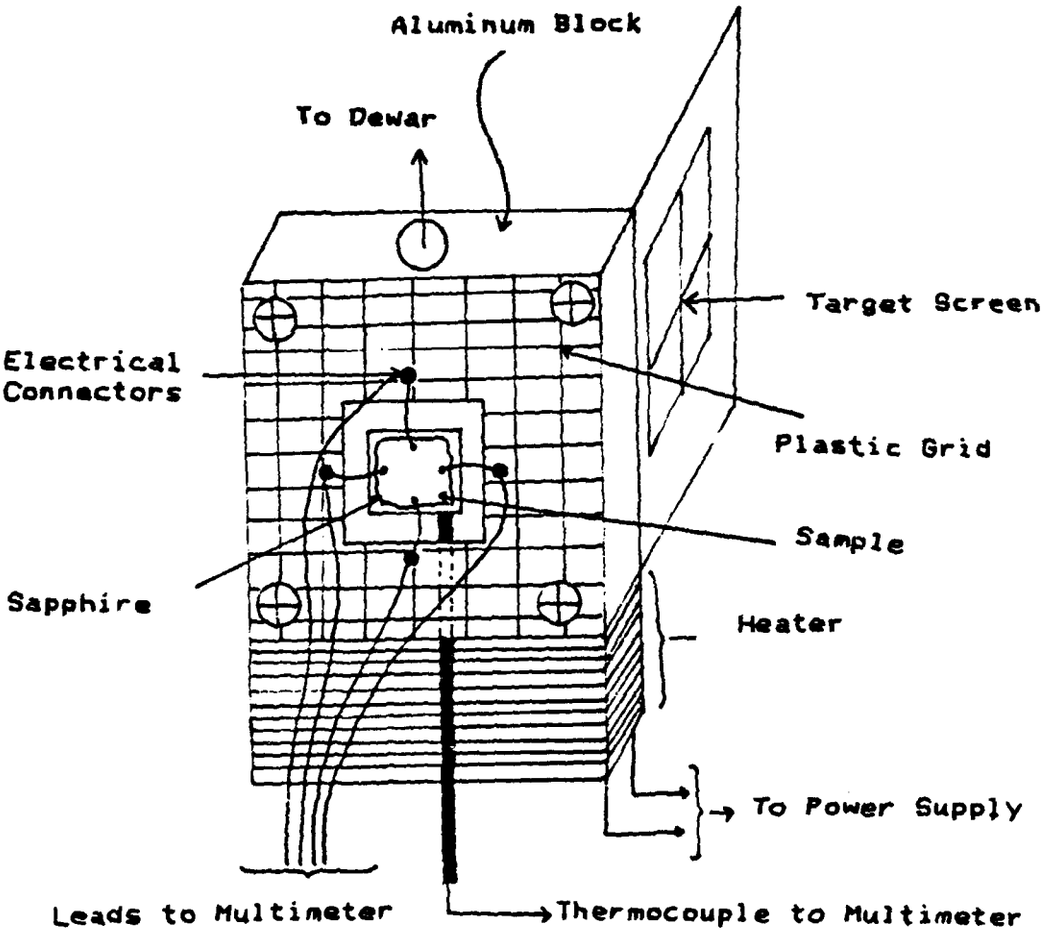

Fig. 6 Apparatus for Mounting Sample in a Vacuum Chamber

was placed on top of the vacuum chamber of the Linac, creating an air tight seal.

The leads from the 4 electrical contacts, the resistive heater, and the thermocouple were led out through the vacuum chamber via a vacuum feedthrough. The heater wire was attached to a 30 volt power supply which was regulated to vary the output of the heater. The thermocouple was connected to a multimeter, which provided a millivolt reading, which could be converted to temperature.

The sample was cooled by introducing liquid nitrogen into the top of the dewar. Temperatures down to about 93°K were obtainable, using this method of cooling. The temperature of the sample was regulated up to room temperature by evacuating the dewar of nitrogen, using an air blower and then regulating the current to the heater. After the required readings were taken, the sample was recooled by placing nitrogen back into the dewar. TV monitors in the Linac control station allowed remote observation of the sample once the dewar was properly aligned. The sample region was marked with grease pencil for future reference and the sample was ready for irradiation.

B. IRRADIATION

The linear accelerator at the Naval Postgraduate School has the capability to accelerate electrons up to a maximum of 100 Mev through a series of three klystrons. For the

semiconductor irradiation studies conducted at NPS to date, 30 Mev electrons have been used, which requires only one of the klystrons to be in operation. The electron beam is focused onto the sample in the vacuum chamber by means of control magnets. The chamber is held at a vacuum of about one microtorr by means of a diffusion pump. The electrons are measured using a secondary emission monitor (SEM). Electrons which strike the SEM cause a capacitor to charge. A voltage integrator measures the voltage which is created by the charging of the capacitor. The amount of voltage is proportional to the charge, and, therefore, the number of electrons per cm^2 can be calculated from the voltage readings.

In order to focus the electron beam without irradiating the sample, the dewar was rotated 90 degrees so that the beam was directed onto the target screen. The beam, after being properly warmed up, was focused onto the region marked in grease pencil on the TV monitor and then shut down. The dewar was rotated back to its original position, placing the sample in direct line with the beam when reactivated. Next the beam was turned on and the sample irradiated to the desired dose. The samples were maintained at temperatures below 95°K during irradiation.

C. POST-IRRADIATION

After the beam was turned off, another set of resistivity readings were taken at about 10 degree intervals covering

temperatures which ranged from 95° to 300°K. A complete set of readings took about 2 hours and reached a final temperature of 300°K. The sample was then recooled to 95° degrees and another complete set of resistivity readings were taken at equivalent temperature intervals to determine the amount of annealing which resulted from the temperature excursions made over the time interval the readings required. Upon completion, the equipment was transported back to the electromagnet lab, the sample remounted to the Hall measurement probe, and post-irradiation Hall measurements were taken at 77°K and 295°K.

In summary, this procedure provided a means of obtaining pre-irradiation, post-irradiation, and post-anneal resistivity values between about 95° to 295°K at 10 degree intervals, and Hall mobility and majority carrier concentrations at 77°K and 295°K before and after irradiation. The data obtained from the experiments will be discussed in Chapter IV.

D. ELECTRON DOSE MEASUREMENTS AND AL BLOCK EFFECTS

As stated earlier, the dose is calculated by the amount of charge produced on a capacitor, which results in a voltage which can be integrated over time. The dose can be converted from volts to electrons per cm^2 by the formula

$$\phi = \frac{CV}{.06qA} \tag{19}$$

where ϕ is the dose, C is the capacitor rating in farads, V is the integrated voltage in volts, q is the charge, A is the area in cm^2, and .06 is a correction factor, since the SEM is only 6% effective in collecting electrons.

The design of the Linac vacuum chamber in which the samples were irradiated is illustrated in Fig. 7. The beam passes through the sample and Al mounting block prior to being sensed by the SEM. Due to the concern over the amount of scattering caused by the 1.2 cm thick Al block, an experiment was conducted to determine the block's effect on dose calculations. During operation two SEMs were used to monitor the beam. One SEM, labelled A in Fig. 7, was connected to a Beckman current monitor which gave an instantaneous measure of the beam intensity and provided a method for keeping the beam tuned to maximum intensity. The other SEM, labelled B in Fig. 7, was connected to the voltage integrator for calculating the dose levels.

The method of conducting this experiment involved integrating to a set voltage level, first without the Al block in the path of the beam and recording the time required, and then recording the time required to obtain the same dose, with the Al block in the path of the beam. It was assumed that the beam remained reasonably constant over the

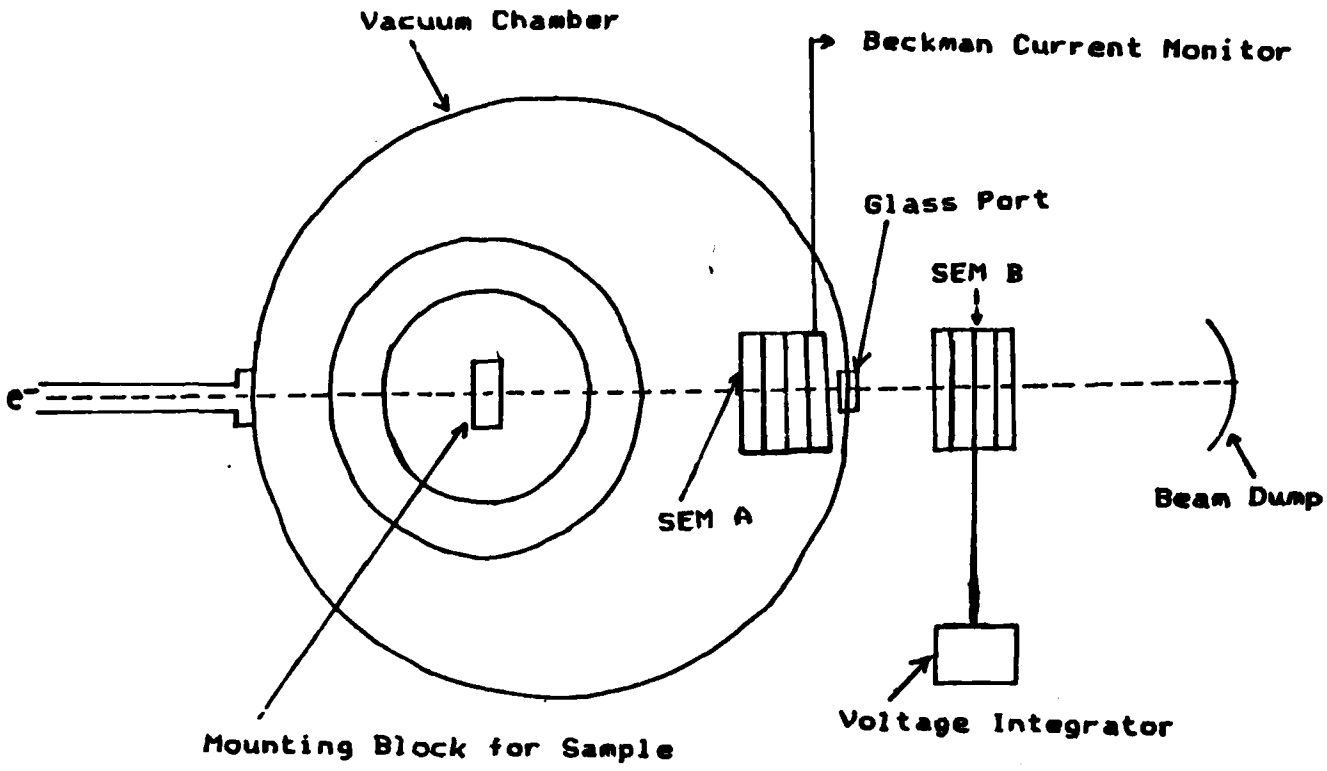

Fig. 7 Vacuum Chamber Arrangement Illustrating location of SEMs and Sample

timeframes required to take the measurements. Nine voltages were chosen, ranging from 1 volt to 60 volts. The times required to achieve these doses ranged from tens of seconds up to a maximum of 12 minutes.

Fig. 8 is a plot of total dose in volts versus time required to reach these doses with and without the block. The difference in times were calculated and this information was used to determine a proper correction factor. The slope of the lines provides the average dose per unit time for the two arrangements; with and without the Al block in the path of the electron beam. The slopes revealed that doses took 1.4 times as long to be reached with the block in the path of the beam compared to measurements without the block in the path of the beam. Since these plots are linear, it can be reasonably assumed that this factor can be used for any dose level. Based on the results of this experiment, all dose levels were increased by a factor of 1.4 when reporting the results of the HgCdTe irradiation experiments.

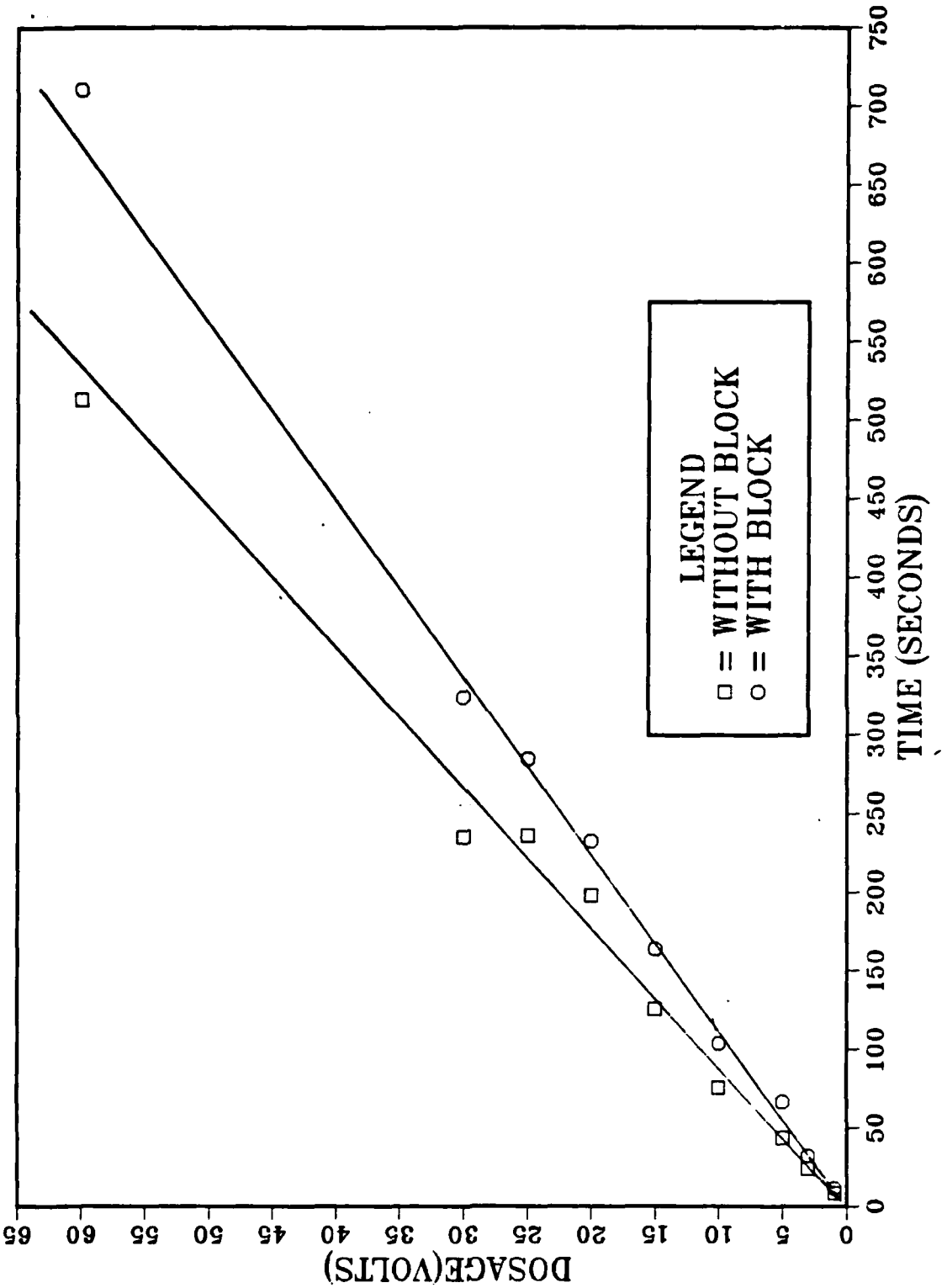

Fig. 8 Dose Level Versus Time for Al Block Experiment

IV. DATA AND ANALYSIS OF HgCdTe IRRADIATION EXPERIMENTS

This chapter contains the data and conclusions of the five irradiation experiments conducted on the HgCdTe samples. All samples used for this experiment were p-type Hg_{1-x} Cd_xTe with an x value of 0.32. In each experiment, irradiation occurred at a constant temperature of about 95°K. Changes in conductivity were monitored over temperatures ranging from 95°K to 300°K. Hall mobility, carrier concentration, and Hall potential difference readings were recorded at 77°K and 295°K.

The purpose of the first experiment was to determine if a significant change in conductivity could be detected as a result of high energy electron irradiation, with the samples held at about 100°K. The first sample irradiated was 5-381 which had a carrier concentration of 4.7×10^{16} e-/cm^2 and mobility of 236 cm^2/$_{v.s}$ at 77°K. Fig. 9 is a graph of conductivity versus temperature between 100° to 240°K for pre-irradiation and dose levels of 4×10^{14} and 4×10^{15} e-/cm^2. As can be seen from the graph, little change was observed for the first dose level of 4×10^{14} e-/cm^2. For the second dose level, which was a order of magnitude higher at 4×10^{15} e-/cm^2, a notable decrease in conductivity was observed, which remained nearly constant over the recorded temperature range.

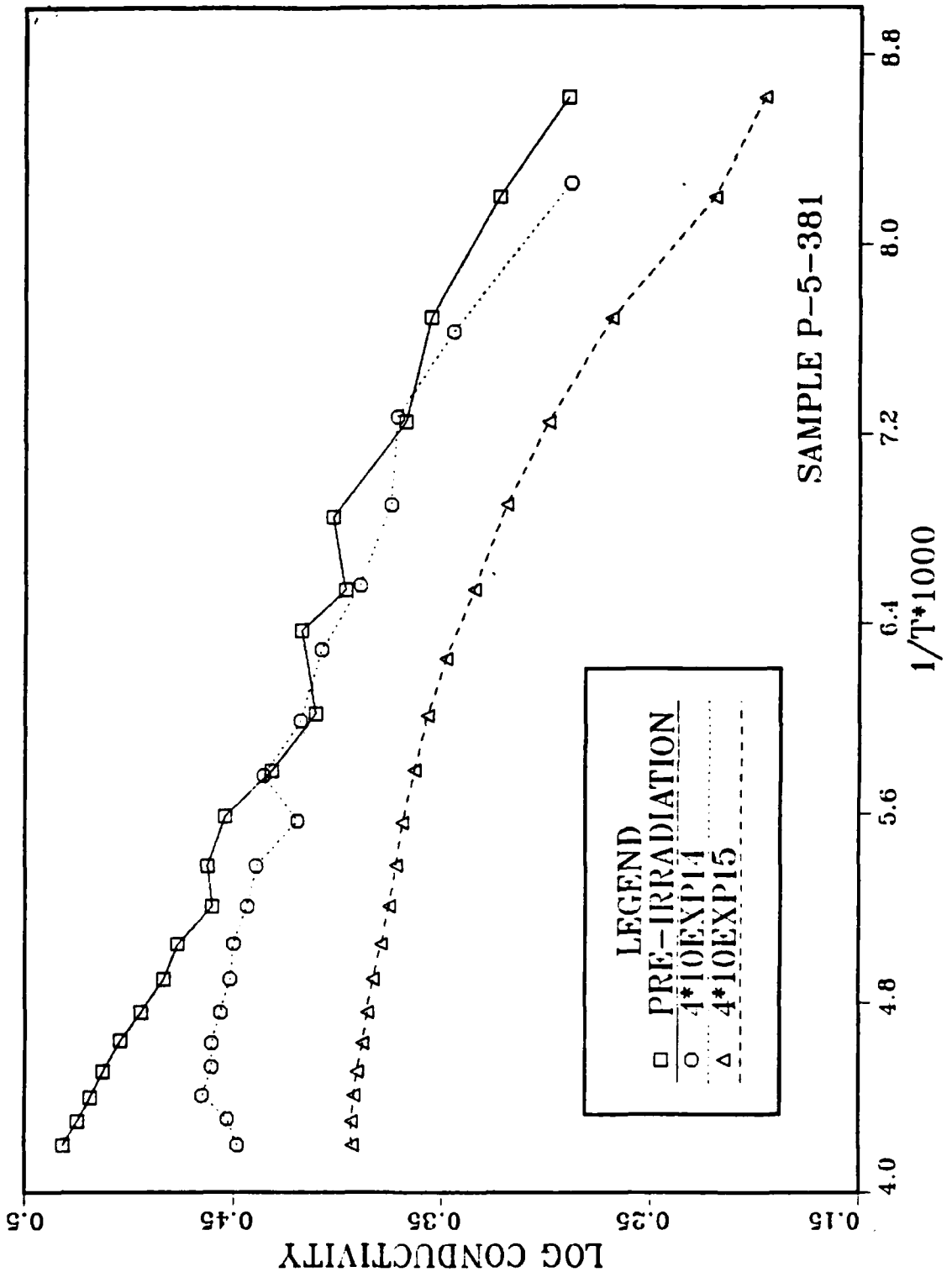

Fig. 9 Determination of Critical Dose Level

Based on the first experiment, a second similar experiment was conducted in order to verify the results. Sample 5-323R was irradiated with a dose level of 4×10^{15} e-/cm^2. Sample 5-323R had a carrier concentration of 4.5×10^{16} e-/cm^2 and a mobility of 240 $cm^2/_{v.s}$ at 77°K prior to irradiation. Fig. 10 is a graph of the results. The post-irradiation conductivity reading at 105°K shows a .882 1/ohms·cm decrease. The difference in conductivity decreases slightly with increasing temperature, reaching a value of .440 1/ohms·cm difference at 166°K which equated to a 50% restoration.

The results of the first two experiments were consistent with Malon et al. (1975) [Ref. 4] who reported decreasing conductivity with increasing dose levels when p-type HgCdTe with a composition variable of $x = 0.20$ was irradiated with 2.5 Mev electrons. The second experiment also revealed a trend towards the conductivity readings approaching their pre-irradiation values as temperature increased. This is a trait which would be observed in later experiments.

Based on the results of the first two experiments, it was decided to expand the scope of the experiments in order to: 1) expand the temperature range to cover temperatures as close to 77°K as attainable up to about 300°K, 2) take conductivity readings over the entire scale, and 3) after taking post-irradiation readings recool the sample and

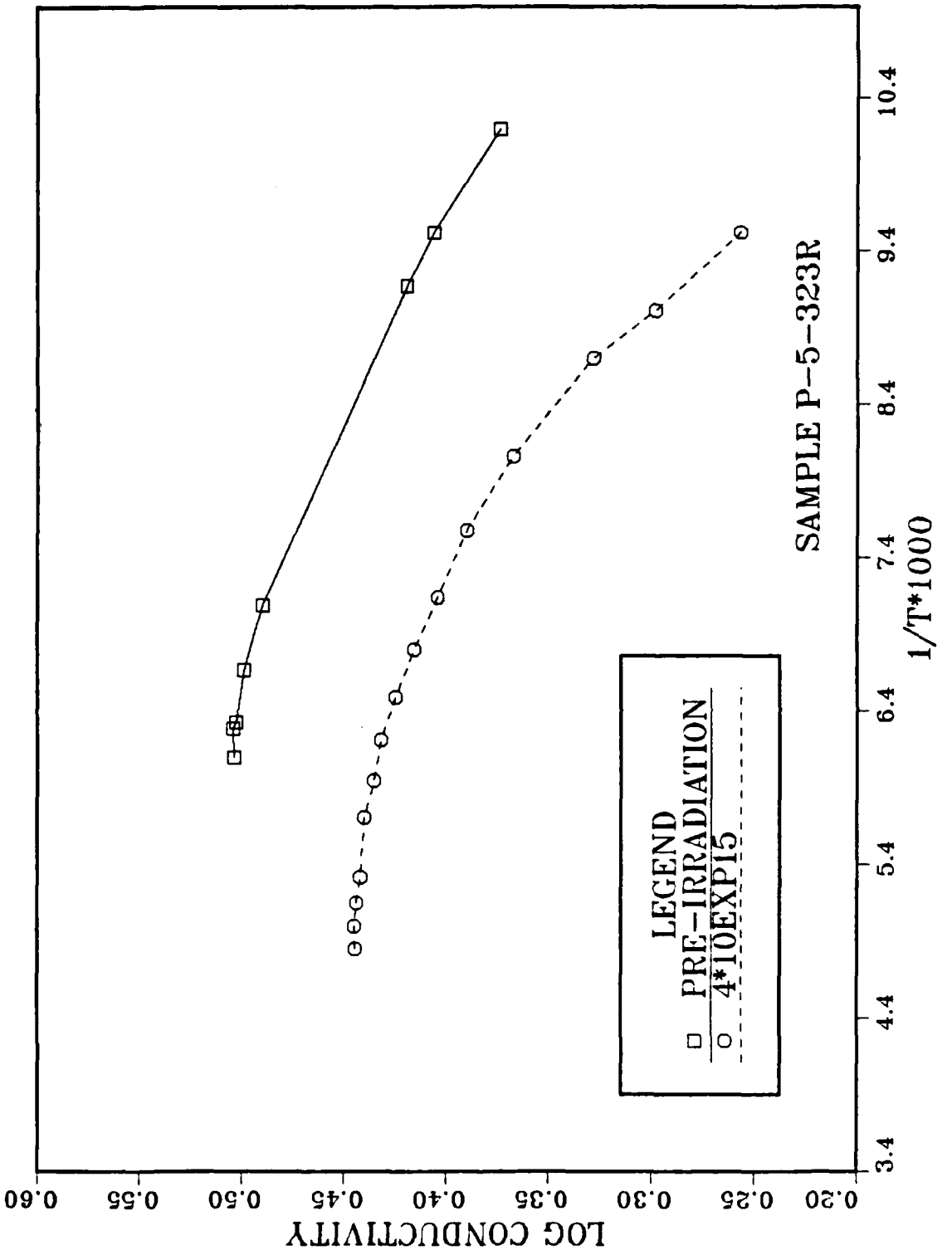

Fig. 10 Verification of Dosage Level

take another complete set of readings to determine the effects of annealing.

The third HgCdTe irradiation experiment was conducted using sample 5-404 which had a carrier concentration of 4.4×10^{16} e-/cm^2 and a mobility of 240 $cm^2/_{v.s}$ at 77°K. The sample was irradiated with a dose of 6×10^{15} e-/cm^2. Fig. 11 is a graph of the pre-irradiation, post-irradiation, and post-anneal results. The post-irradiation conductivity at 100°K shows a decrease of 1.8 1/ohm·cm which increases to a maximum difference of 2.7 1/ohms·cm at 125°K and then steadily increases to almost its original value at 300°K. Post-anneal measurements indicated a conductivity change of about 25% at 100°K with a distinctive dip at the same place as the post-irradiation curve. Again, for the post-anneal plot the conductivity readings steadily increase and return to near their pre-irradiation values at room temperature.

The results of the pre-irradiation and post-irradiation Hall mobility, Hall potential difference, and carrier concentration at 77°K and 295°K are listed in Table 1. An examination of the data reveals that the Hall potential difference has changed sign at 295°K after irradiation of sample 5-404. The change of sign indicates a p to n-type conversion has occurred at some temperature below 295°K. As temperature decreased to 77°K, the sample was once again found to be p-type, as indicated by the positive Hall potential difference. The mobility increased by a factor

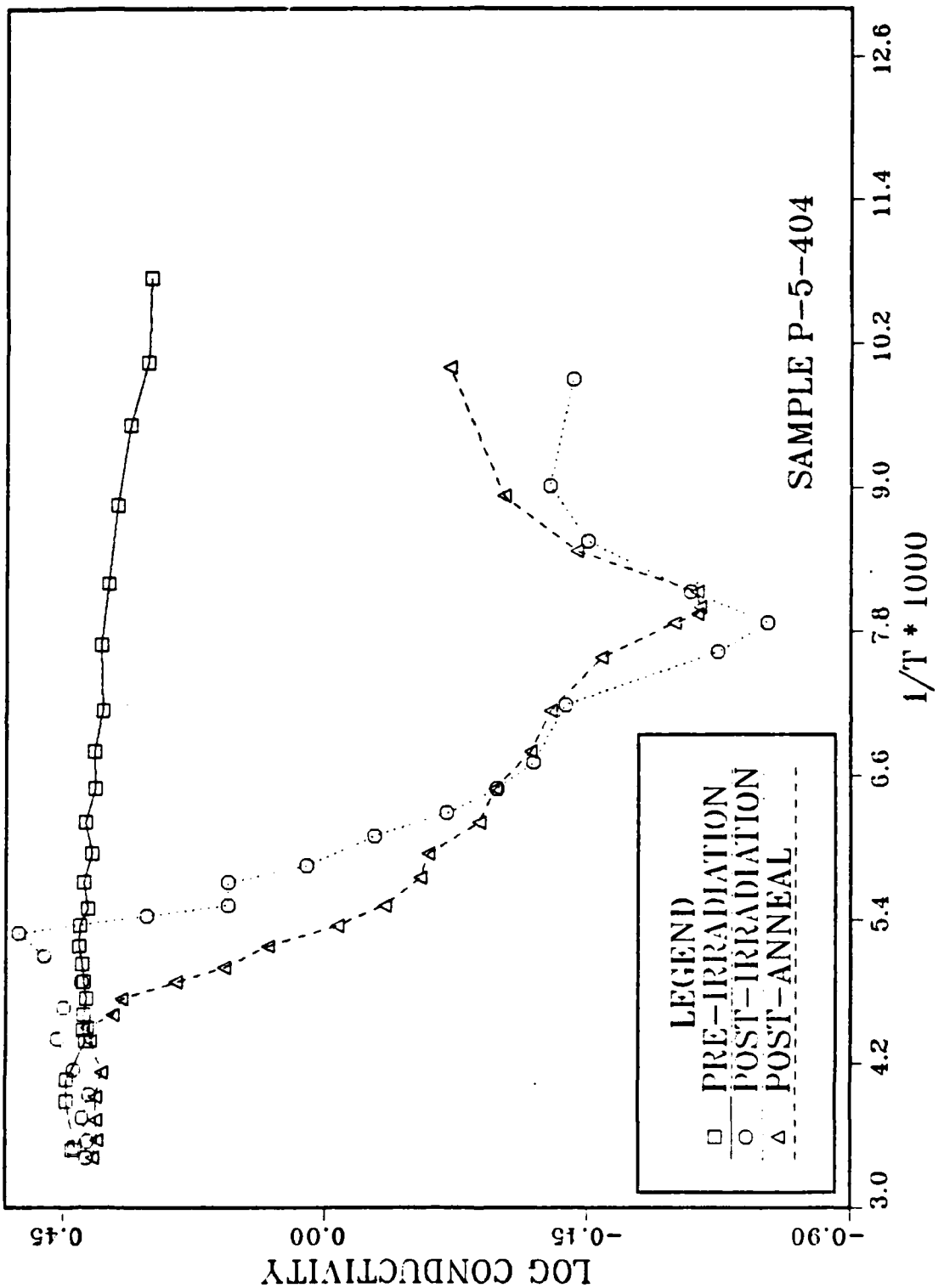

Fig. 11 High Dose Level Effects

TABLE 1

RESULTS OF MOBILITY, MAJORITY CONCENTRATION AND TYPE AT 77°K AND 295°K FOR EXPERIMENTS 3, 4, AND 5.

Sample Number	Dose in electrons per cm^2	Temp in ^oK	Mobility in cm^2 per v.sec		Post-irrad Type Majority *	Majority Carrier Concentration in cm^{-3}	
			Pre-Irrad	Post-Irrad		Pre-Irradiation	Post-Irradiation
P-5-404	6×10^{15}	77	240	99	P	4.5×10^{16}	6.3×10^{16}
		295	40	264	N	4.1×10^{17}	5.0×10^{16}
P-5-528L	6×10^{15}	77	202	45	P	7.1×10^{16}	8.6×10^{16}
		295	52	170	N	3.8×10^{17}	5.6×10^{16}
P-5-531	2×10^{15}	77	243	251	P	3.1×10^{16}	2.7×10^{16}
		295	64	38	N	1.6×10^{17}	2.3×10^{17}

*Note: All samples are p-type at 77° and 295° for pre-Irradiation Measurements

of about 6, while the carrier concentration decreased by an order of magnitude.

The fourth HgCdTe irradiation experiment was conducted using sample 5-528L which had a carrier concentration of 7.4×10^{16} e-/cm^2 and a mobility of 188 $cm^2/_{v.s}$ at 77°K. For this experiment the dose levels were increased in increments and the conductivity recorded at 95°K after each irradiation run. As shown in Fig. 12, a steady decrease in conductivity resulted from successively higher doses. At the maximum dose of 6×10^{15} e-/cm^2 the conductivity had decreased by about 1.8 1/ohms·cm at 95°K. A post-anneal reading of 95°K revealed a 25% restoration of the decrease in conductivity. This 25% restoration is equivalent to the annealing recorded for sample 5-404 in experiment 3.

The Hall potential difference, Hall mobility, and carrier concentration for 5-528L, Table 1, reveal the same trends as with sample 5-404, only to a lesser degree. The post-irradiation Hall potential difference at 295°K was negative, indicating that type conversion had taken place. At 295°K the Hall mobility increased by a factor of 3 while the carrier concentration decreased by a factor of 7. As the temperature decreased to 77°K, the sample reverted to p-type.

Observation of samples 5-404 and 5-528L after irradiation at high dose levels revealed a bluish discoloration of the surface of the sample around the area that the beam

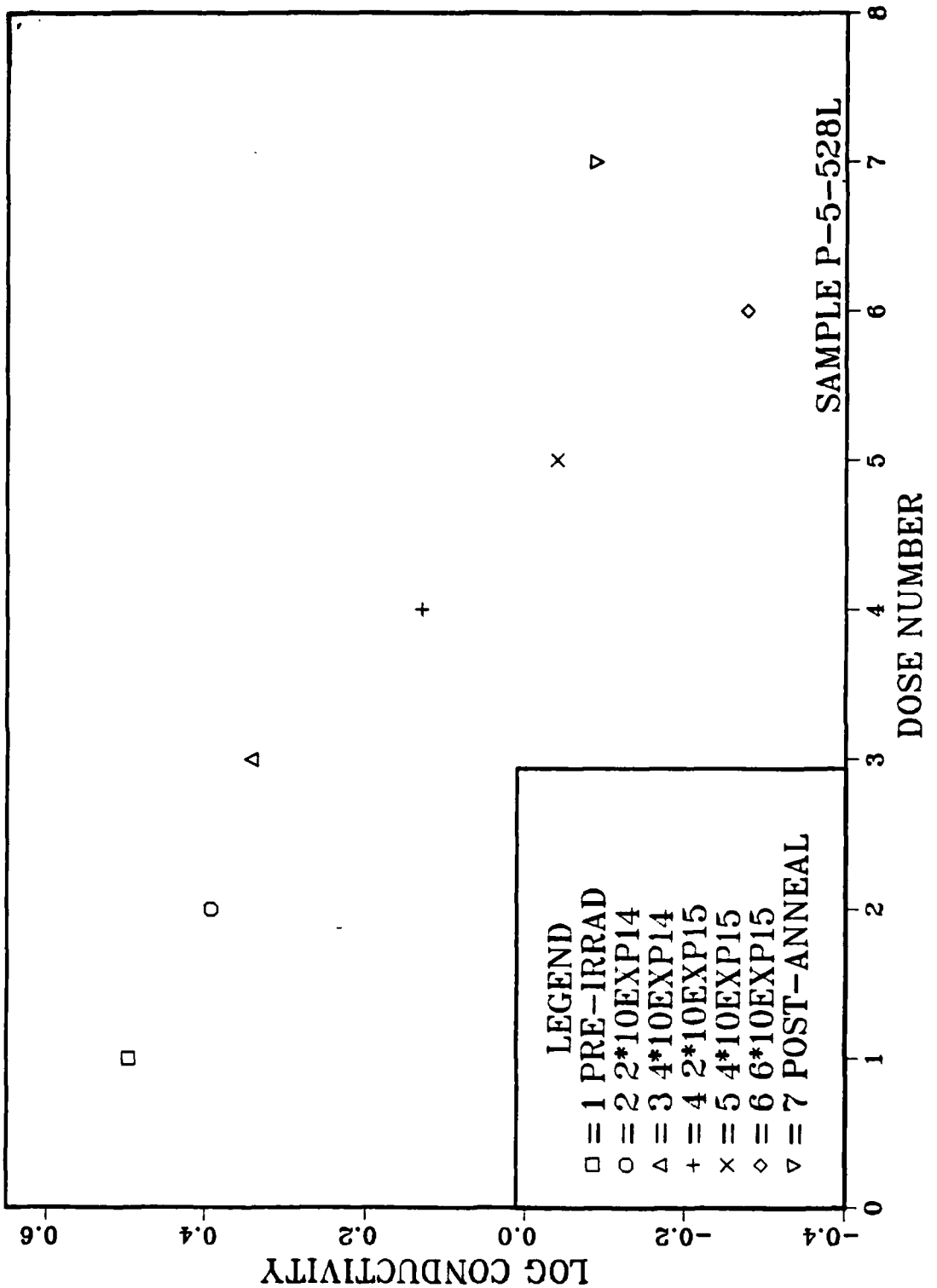

Fig. 12 Effects of Increasing Dose Levels

was focused upon. This discoloration appeared to fade over a period of time after irradiation ceased. This bluish discoloration may have been a result of mercury evaporating to the surface, due to the heat generated by the electron beam. [Ref. 12] Some brownish discoloration remained permanently and is typical of samples which have been irradiated. [Ref. 13]

A model which explains the behavior reported on samples 5-404 and 5-528L follows. As explained earlier, an acceptor level is created by annealing in a Te-rich vapor which creates a p-type material. An acceptor level of about 20 mev above the valence band has been reported for p-type material, with x values between 0.2 to 0.5. [Ref. 6] It is hypothesized that the electron irradiation creates donor defect levels below the conduction band which contribute electrons to the conduction band. Malon et al. (1975) [Ref. 4], Melngailis (1972) [Ref. 3], and Voiitsekhovskii (1981) [Ref. 5] have all reported the creation of donor defects as a result of electron irradiation of p-type HgCdTe. Fig. 13 illustrates a p-type material in which donor defects exist. Malon et al. (1975) [Ref. 4] showed that the statistical behavior of the electron irradiation induced states in p-type material can be described by two defect levels, an acceptor level in the bandgap directly above the valence band, and a donor level above the conduction band. [Ref. 6] If enough of these donor defect

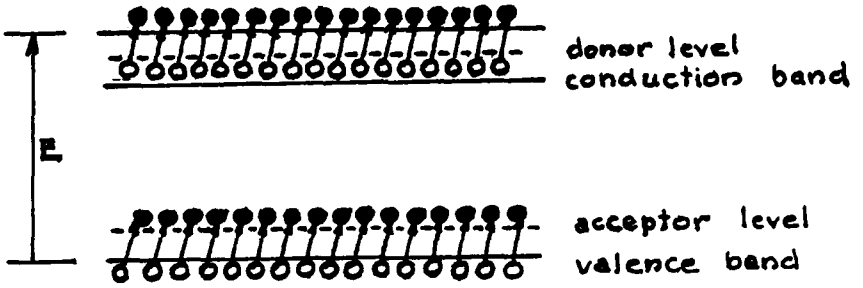

Figure 13. Donor and Acceptor Levels in a Semiconductor Material

levels are created, the electrons will outnumber the holes, become the majority carriers, and cause n-type conversion. As the temperature decreases, a point is reached whereby the donor defects freeze out, which means they no longer have enough thermal energy to reach the conduction band, and become ineffective. This allows the holes to once again become the majority carriers, and the material reverts to p-type.

The mobility, after type conversion to n-type, increases despite the carrier concentration decreasing since electrons are typically 1000 times more mobile than holes. Therefore even though only 10% as many carriers are measured, a 6 fold increase in mobility occurs.

An example of a minimum conductivity phenomenon, existing at 125°K occurs, in Fig. 11. It is hypothesized that this temperature equates to a major donor defect level which results in the p to n-type conversion. Multiplying this temperature 125°K, by Boltzmann's constant yields an energy level of 10.8 mev. Converting this value to wavelength yields 115 micrometers. Verification of this defect level using optical methods would place this hypothesis on firm ground. However, equipment to accomplish this is not currently available at NPS.

The last irradiation of HgCdTe experiment was conducted to determine the results of low dose irradiation on annealing. Sample 5-531 had a carrier concentration of 3×10^{16} e-/cm^2 and a mobility of 246 cm^2/$_{v.s.}$ at 77°K. The sample was irradiated with 4 doses starting at 4×10^{13} e-/cm^2 and ending with a max dose of 2×10^{15} e-/cm^2. Fig. 14 is a graph of the results of experiment 5. Conductivity decreased at 95°K as the dose levels increased. At the maximum dose of 2×10^{15} e-/cm^2, the conductivity had decreased by 2.2 1/ohms·cm. The difference decreased with rising temperature, returning to almost its pre-irradiation value at 300°K. The post-anneal conductivity shows a 75% restoration of the conductivity decrease at 95°K compared to a value of 25% reported for the experiments

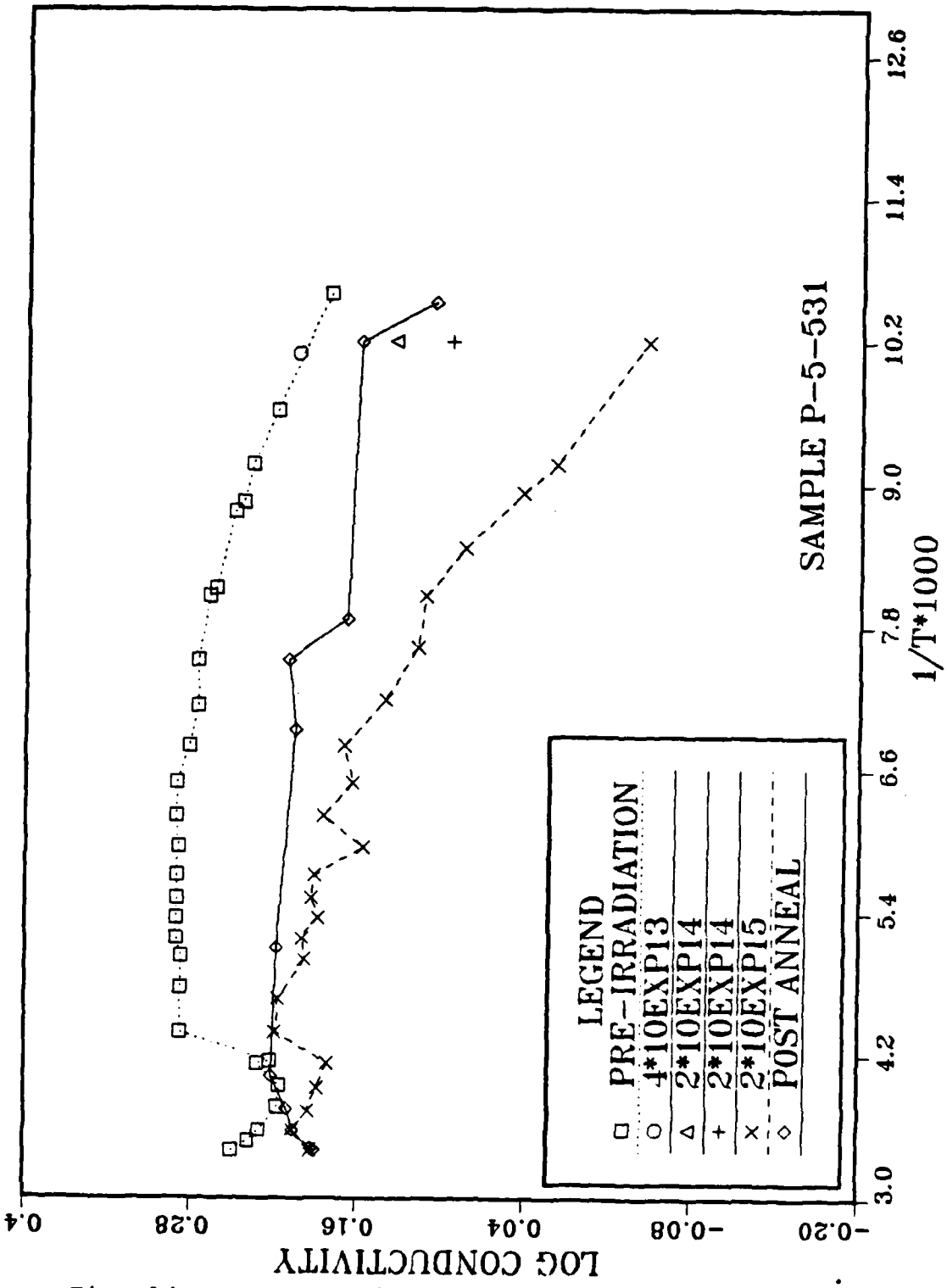

Fig. 14 Low Dose Effect on Annealing at 95°K

on samples 5-404 and 5-528L which used higher dose levels. This indicates that the damage caused by the lower dose beam probably was less permanent in nature than that from the higher dose beam.

The post-irradiation Hall potential difference, Hall mobility, and carrier concentration, listed in Table 1, did not follow the trends reported in the 2 previous experiments except that p to n-type conversion at 295°K did take place.

A possible explanation of these puzzling results may be that this sample has two carrier conduction. The carrier concentrations of holes and electrons are comparable, whereas the formulas which were used to calculate these quantities assume that one carrier concentration is much larger than the other. If the absolute value of the Hall potential difference, Table 1, is compared with the same values for the higher dose level experiments, it is seen to be considerably less. Therefore, this sample is closer to the region where two carrier effects are dominating and the data analysis becomes inapplicable. As the absolute value of the Hall potential becomes greater, the one carrier effects begin to dominate, the equations become valid and the expected results are observed, as was the case in experiments 3 and 4. Malon et al. (1975) [Ref. 4] reported similar results and conclusions for regions in mobility versus temperature and carrier concentration versus temperature curves. These curves exhibited steep increases

and decreases, respectively, around the temperatures where conversion took place.

V. CONCLUSIONS AND RECOMMENDATIONS

It can be concluded from this research that 30 Mev electron irradiation causes defect damage to p-type HgCdTe which results in a reduction in the material's conductivity. In general this reduction in conductivity is larger for low temperatures around 95°K and becomes less as the temperature increases to 300°K. An exception to this rule occurred around 125°K for one sample. Some of this damage was temporary, as shown by partial annealing at room temperature. Other damage was permanent, as evidenced by the permanent p to n conversion at 295°K, which took place in each experiment when doses were above about 1×10^{15} e-/cm^2.

Although not proven by the experiments reported here, it is reasonable to conclude that donor defects are responsible for the observed alterations in electrical properties. This hypothesis is consistent with the experimental results and conclusions of other comparable electron irradiation studies summarized in Chapter I and discussed in Chapter IV.

Lifetimes for p-type HgCdTe are very short and difficult to measure. Lifetime and photoluminescence measurements which could shed light on the actual damage mechanisms require pulsed lasers with 10 nanosecond resolution. Currently, equipment capable of taking these measurements is not available at NPS or Rockwell Science Center, Thousand

Oaks. It is however expected that Rockwell will develop this capability in the future. [Ref. 14]

The Linear Accelerator located at NPS makes this location an ideal place for conducting electron irradiation studies. A worthwhile thesis project at NPS would be to develop a more sophisticated irradiation laboratory capable of taking carrier concentration and mobility readings over the entire temperature range and at all dose levels during the experiment. Suggestions for building an irradiation lab are: 1) mount an electromagnet or a permanent magnet capable of 2-4 KGauss inside the Linac vacuum chamber, 2) obtain a commercially available liquid nitrogen dewar capable of achieving temperatures close to 77°K, 3) redesign the base of the dewar so that the sample can be remotely rotated between the poles of the magnet, 4) obtain a temperature controller which could be programmed via a computer to automatically raise and hold the temperature of the sample constant while readings are recorded. These improvements to the existing lab would eliminate most of the difficulties experienced during irradiation studies conducted to date at NPS, and coupled with the developing capability to measure lifetime and photoluminescence by Rockwell, would greatly enhance the study of high energy electron irradiation effects on p-type HgCdTe.

LIST OF REFERENCES

1. Ness, C.Q., Electron Irradiation of Light Emitting Diodes, Master's Thesis, Naval Postgraduate School, Monterey, CA, 1984.

2. Bauer, C.P., Electron Irradiation of n-type Cadmium Telluride, Master's Thesis, Naval Postgraduate School, 1985

3. Melngailis, J., Ryan, J.L., Harman, T.C., "Electron Radiation Damage and Annealing of $Hg_{1-x}Cd_xTe$ at Low Temperatures," J. Appl. Phys. Vol. 44, No. 6, June 1973.

4. Mallon, C.E., Green, B.A., Leadon, R.E., Naber, J.A., Study of the Effects of Radiation on the Electrical and Optical Properties of HgCdTe, Air Force Cambridge Research Lab., Intelcom Rad Tech. 8027-019, 1975.

5. Voitsekhovskii, A.V., Lilenko, Yv. Vo, Kokhanenko, A.P., Petrov, A.S., "High Temperature Electron Irradiation and Isochyonal Annealing of P-HgCdTe Crystals," Radiation Effects," J. Appl. Phys. Vol. 66, pp. 79-84, 1981.

6. Dornhaus, R., Nimtz, G., The Properties and Applications of the $Hg_{1-x}Cd_xTe$ Alloy System, Springer Tracts in Modern Physics, Springer-VerLag, New York, 1976.

7. Hudson, R.D., Infrared System Engineering, Wiley, New York, 1969.

8. Willardson, R.K., Beer, A.C., Semiconductors and Semimetals, Academic Press, New York, 1981.

9. Van der Pauw, L.J., "A Method of Measuring Specific Resistivity and Hall Effect of Discs of Arbitrary Shape, Phillips Research Reports 13, 1-9, 1958.

10. Muller, R.S., Kamins, T.I., Device Electronics for Integrated Circuits, Wiley, New York, 1977.

11. Edwall, D.D., Gertner, E.R., Tennant, W.E., Liquid Phase Epitaxial Growth of Large Area $Hg_{1-x}Cd_xTe$ Epitaxial Layers, Rockwell International Science Center, Thousand Oaks, 1983.

12. Newman, P., Rockwell International Science Center, Private Communication, May 1985.

13. Edwell, D.D., Rockwell International Science Center, Private Communication, May 1985.

INITIAL DISTRIBUTION LIST

		No. Copies
1.	Defense Technical Information Center Cameron Station Alexandria, Virginia 22304-6145	2
2.	Library, Code 0142 Naval Postgraduate School Monterey, California 93943-5100	2
3.	Dr. K. C. Dimiduk, Code 61Dm Physics Department Naval Postgraduate School Monterey, California 93943-5100	6
4.	Dr. D. L. Walters, Code 61We Physics Department Naval Postgraduate School Monterey, California 93943-5100	1
5.	Dr. G. E. Schacher, Code 61Sq Physics Department Naval Postgraduate School Monterey, California 93943-5100	2
6.	Dr. Paul Newman, Manager Materials Development Technology Science Center 1049 Camino Dos Rios P. O. Box 1085 Thousand Oaks, Ca 91360	2
7.	LCDR Dennis G. Morral, USN 127 School Lane Souderton, Pa 18964	1

END

FILMED

11-85

DTIC